Proceedings of the International Association for Shell and Spatial Structures (IASS) Symposium 2010, Shanghai
Spatial Structures – Permanent and Temporary
November 8-12 2010, Shanghai, China

Configuration optimization of clamping members of frame-supported membrane structures

Taku NAKAJIMA[1], Makoto OHSAKI[2*], Jun FUJIWARA[3], Fumiyoshi TAKEDA[3]

[1]Dept. of Architecture and Architectural Engineering, Kyoto University, Japan

[2*]Dept. of Architecture, Hiroshima University,
1-4-1, Kagamiyama, Higashi-Hiroshima 739-8527, Japan
ohsaki@hiroshima-u.ac.jp

[3]Technical Research Center, Taiyo Kogyo Corporation, Japan

Abstract

A method is presented for configuration optimization of frames that have specified properties on nodal displacements, stresses, and reaction forces against static loads. The conventional ground structure approach is first used for topology optimization. An optimal topology with a small number of members is obtained by assigning artificially small upper-bound displacement. The nodal locations and cross-sectional areas are next optimized under stress constraints. The proposed method is applied to design of self-fastening clamping members for membrane structures modeled using frame elements. An optimization result is also presented for a clamping member that adjusts deformation of membrane by applying a clamping force with a vertically attached bolt.

Keywords: Membrane structure, Clamping member, Configuration optimization, Stress constraints

1 Introduction

There are many researches on simultaneous optimization of shape and topology, which is called *configuration optimization*, of trusses and frames [1-4]. Optimal topologies of trusses under constraints on global properties such as compliance and displacements can be easily obtained using the standard ground structure approach, where unnecessary members are removed through optimization from a highly-connected ground structure.

However, there still exist several difficulties in problems under stress constraints [5-7], which are categorized as local constraints [8] that lead to existence of many thin members or elements; i.e., the number of members cannot be reduced effectively by simple application of the ground structure approach. In the most widely used SIMP (*solid isotropic microstructure with penalty* or *solid isotropic material with penalization*) approach [9,10] to topology optimization of continua, an intermediate value of material density is penalized by assigning artificially small stiffness.

Membrane structures are generally connected to the boundary frames with clamping members as illustrated in Figure 1. Since such devices are mass-products and have large portion of the total weight of the membrane structure, it is possible that the total production cost can be reduced by optimizing shapes and cross-sectional properties of the members. Furthermore, when external loads such as wind loads are applied to the membrane, its tensile force increases and the membrane sheet may detach from the clamping member prior to the fracture of membrane material. Therefore, the load resistance capacity of the membrane structure can be improved by optimizing the clamping members so that the clamping force increases as a result of the increase of tensile force of the membrane.

In this study, we present a method for design of clamping members of frame supported membrane structures. The clamping members are modeled using frame elements. The objective function is the total structural volume, which is to be minimized, and the constraint is given for the clamping force against the membrane to obtain a self-fastening member. We also present an optimization result of a clamping member that enables us to adjust deformation of membrane by applying a clamping force through a vertically attached bolt.

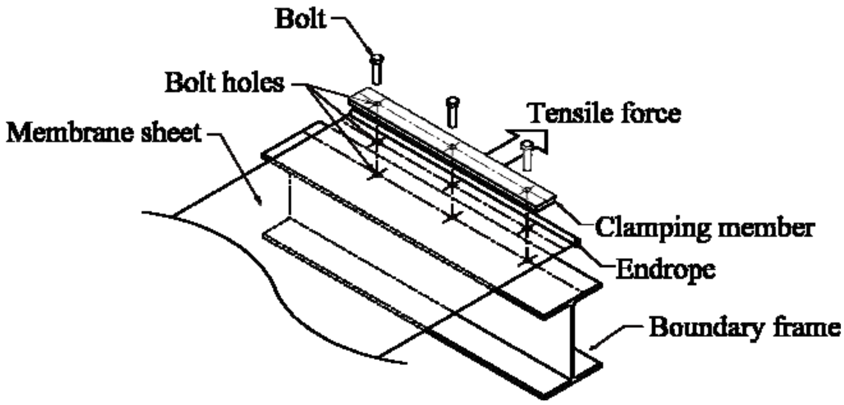

Fig. 1: Illustration of a clamping member of a frame-supported membrane structure

2 Overview of tensioning process and clamping member of a frame-supported membrane structure

We first describe overview of tensioning process as illustrated in Figure 2. In this process, temporary supports are attached first to the structural boundary members along the boundary of the membrane sheet. To obtain reaction force from the boundary frames through the temporary support, the membrane is pulled (tensioned) by using a tool until the preassigned holes of the membrane are located on the bolt holes of the boundary frame. Finally, the membrane is pressed to the frame using the clamping member and bolts. However, in this process, there exist the following difficulties:

1. Adjustment of tensile force of membrane is very difficult because the holes are preassigned in the factory.
2. Temporary supports for obtaining reaction force through tensioning tools are needed in addition to the boundary frame.

In the following, optimization approaches are presented to overcome these difficulties. The section of the clamping member is modeled as a frame with small elastic deformation.

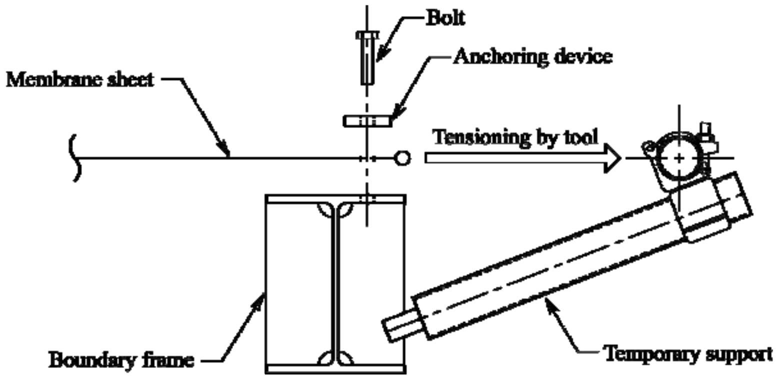

Fig. 2: Construction process of a frame-supported membrane structure

3 Topology optimization of a self-fastening clamping member

3.1 Problem formulations

Optimization of topology, cross-sectional areas of members, and nodal locations, which is simply called configuration optimization, is carried out for a frame subjected to static loads. The standard ground structure approach is used at the first step; i.e., unnecessary nodes and members are removed through optimization from the highly connected initial ground structure. The design variables are the cross-sectional areas $\mathbf{A} = (A_1, \dots, A_m)^{\mathrm{T}}$ of members, where m is the number of members in the ground structure. The cross-sectional properties such as the second moment of inertia and the section modulus are assumed to be functions of the cross-sectional area.

A constraint is given so that the maximum absolute value $|\sigma_i(\mathbf{A})|$ among the stresses at the two edges of two ends of the ith member is less than the specified upper bound σ^{U}. A lower bound R^{L} is also given for the reaction force $R(\mathbf{A})$ at the specified direction of a support. Then the optimization problem for minimizing the total structural volume $V(\mathbf{A})$ is formulated as

$$\begin{aligned} \text{P1:} \quad & \text{minimize} && V(\mathbf{A}) && \text{(1a)} \\ & \text{subject to} && |\sigma_i(\mathbf{A})| \le \sigma^{\mathrm{U}} \quad (i = 1, \dots, m) && \text{(1b)} \\ &&& R(\mathbf{A}) \ge R^{\mathrm{L}} && \text{(1c)} \\ &&& \mathbf{A}^{\mathrm{L}} \le \mathbf{A} \le \mathbf{A}^{\mathrm{U}} && \text{(1d)} \end{aligned}$$

where $\mathbf{A}^{\mathrm{L}} = (A_1^{\mathrm{L}}, \dots, A_m^{\mathrm{L}})^{\mathrm{T}}$ and $\mathbf{A}^{\mathrm{U}} = (A_1^{\mathrm{U}}, \dots, A_m^{\mathrm{U}})^{\mathrm{T}}$ are the lower and upper bounds for $\mathbf{A}$. Note that a small positive value is given for the lower-bound cross-sectional area to prevent instability of the frame during optimization process, and the member with $A_i = A_i^{\mathrm{L}}$ is removed after optimization.

An optimal topology satisfying constraints on stresses and a reaction force may be found by solving Problem P1, which is a standard nonlinear programming (NLP) problem. It is well known in truss topology optimization that the number of members cannot be successfully reduced by using a conventional ground structure approach with an NLP algorithm if stress constraints are considered [6,7]. Therefore, we first carry out optimization, as follows, with a displacement constraint and without stress constraint:

$$\text{P2:} \quad \text{minimize} \quad V(\mathbf{A}) \tag{2a}$$
$$\text{subject to} \quad |U(\mathbf{A})| \le U^{\mathrm{U}} \quad (i=1,\ldots,m) \tag{2b}$$
$$R(\mathbf{A}) \ge R^{\mathrm{L}} \tag{2c}$$
$$\mathbf{A}^{\mathrm{L}} \le \mathbf{A} \le \mathbf{A}^{\mathrm{U}} \tag{2d}$$

where U^{U} is the upper bound for the absolute value of a specified displacement component *U*. Problem P2 is first solved to obtain a topology with a small number of members. Then Problem P1 is solved starting with the optimal solution of Problem P2 to obtain an approximate optimal topology under constraints on stresses and a reaction force.

Finally, the nodal locations as well as the cross-sectional areas are optimized to obtain the optimal configuration under constraints on stresses and a reaction force. Optimal solution of Problem P2 can be used as the ground structure with reduced number of members. Suppose we use Problem P2, and, consequently, $\mathbf{A}$ and *m* denote the cross-sectional areas and the number of members of the ground structure with a reduced size. Let **X** denote the vector consisting of the variable components of the nodal coordinates. Then the optimization problem is formulated as

$$\text{P3:} \quad \text{minimize} \quad V(\mathbf{A},\mathbf{X}) \tag{5a}$$
$$\text{subject to} \quad |\sigma_i(\mathbf{A},\mathbf{X})| \le \sigma^{\mathrm{U}} \quad (i=1,\ldots,m) \tag{5b}$$
$$R(\mathbf{A},\mathbf{X}) \ge R^{\mathrm{L}} \tag{5c}$$
$$\mathbf{A}^{\mathrm{L}} \le \mathbf{A} \le \mathbf{A}^{\mathrm{U}} \tag{5d}$$
$$\mathbf{X}^{\mathrm{L}} \le \mathbf{X} \le \mathbf{X}^{\mathrm{U}} \tag{5e}$$

where $\mathbf{X}^{\mathrm{L}}$ and $\mathbf{X}^{\mathrm{U}}$ are the lower and upper bounds for **X**, respectively.

In the following examples, optimization is carried out using the software library SNOPT Ver. 7.2 [11] utilizing sequential quadratic programming. The sensitivity coefficients are computed by using a finite difference approach. The best solution from ten different initial solutions is taken as an approximate optimal solution.

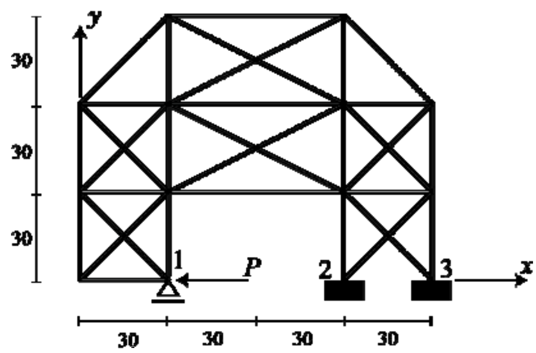

Fig. 3: A frame model (Type 1)

3.2 Numerical examples

We first find the overall configuration of the device that automatically clamps the membrane as the result of introducing tensile force to the membrane sheet. Consider a frame (Type 1) as shown in Figure 3 as the ground structure, where the intersecting diagonal members are rigidly connected at the centers. The frame is supported with roller at support 1 and fixed at supports 2 and 3. The member is supposed to have solid rectangular section with the fixed width $b = 10$ mm. A load $P = 500$ N is applied in the negative *x*-direction at support 1. Problem P1 is first solved for finding an optimal topology, where *R* represents the vertical (positive *y*-directional) reaction force at support 1; i.e., the device clamps the membrane if *R* is positive.

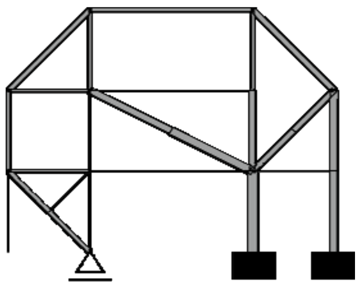

Fig. 4: Optimal configuration of Type 1 with stress constraints

The elastic modulus of the members is 2.0×10^5 N/mm. The lower bound R^{L} for reaction force is 200 N. The cross-sectional areas of all the 42 members are independent variables with lower bound $A_i^{\mathrm{L}} = 0.1$ mm^2, whereas different values of A_i^{U} are used for the optimization problems below. The upper-bound stress is $\sigma_i^{\mathrm{U}} = 200$ N/mm^2. In the following, the units of length and force are mm and N if they are not explicitly specified. A uniform random number $0 \le r_i < 1$ is generated to obtain the initial value of A_i as $50r_i + 1.0$.

Problem P1 is solved with the upper-bound cross-sectional area $A_i^{\mathrm{U}} = 200$; i.e., the maximum height is $200/10 = 20$. The optimization result after removing the members with $A_i = A_i^{\mathrm{L}}$ is shown in Figure 4, where the height of each member is drawn with real scale. Note that the reaction constraint is active as $R^{\mathrm{L}} = 200$, and the objective function value is $V = 1.1018\times10^4$. If all cross-sectional areas have the same value 100, then $R = -141.11$; i.e., the device should be pulled downward by the membrane sheet at support 1, which is not realistic; therefore, the direction of reaction force has been successfully reversed through optimization.

As is seen from Figure 4, the number of members is not drastically reduced, because stress constraints should be satisfied in all members including very thin members. Therefore, Problem P2 is next solved to obtain a topology with smaller number of members. A large upper bound $A_i^{\mathrm{U}} = 1000$ is given to allow the existence of thick members. The upper bound $U^{\mathrm{U}} = 0.1$ is given for the absolute value of the horizontal displacement of support 1. The optimal topology is shown in Figure. 5(d), where the height of each member is scaled by 1/5. The optimal objective value is $V = 1.6781 \times 10^4$. As is seen from Figure. 5(d), there still exist many members that seem to be unnecessary.

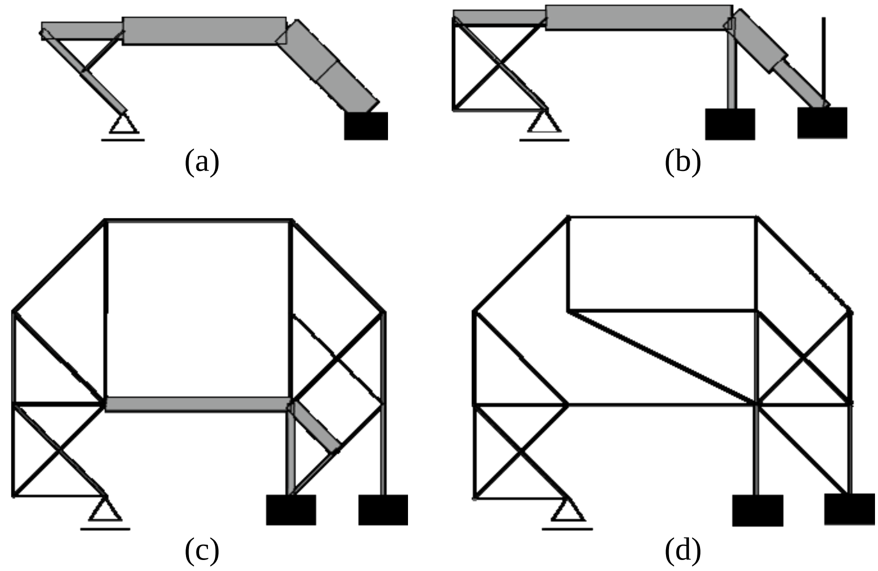

Fig. 5: Optimal topology of Type 1 for various values of U^{U}*; (a)* $U^{\mathrm{U}} = 0.01$*, (b)* $U^{\mathrm{U}} = 0.02$*, (c)* $U^{\mathrm{U}} = 0.04$*, (d)* $U^{\mathrm{U}} = 0.1$

Table 1: Total structural volume V and number of members n^{opt} *of optimal topology of Type 1 for various values of* U^{U}

U^{U}	V	n^{opt}
0.1	16782	30
0.09	18513	30
0.08	23396	27
0.07	23516	30
0.06	27289	30
0.05	32310	28
0.04	38090	28
0.03	46826	29
0.02	50352	12
0.01	67593	7

Therefore, we assign smaller upper-bound displacement to allow larger structural volume and cross-sectional areas. The optimal solution for $U^{\mathrm{U}} = 0.01$ is shown in Figure 5(a), where $V = 6.7593 \times 10^4$ and the height of each member is scaled by 1/5. The solutions for $U^{\mathrm{U}} = 0.02$ and 0.04 are also shown in Figures 5(b) and (c), respectively. We can confirm from Figures 5(a)-(d) that the number of members decreases and the heights of existing members increase as the displacement constraint becomes tight.

The total structural volume V and number of members n^{opt} of optimal topology for various values of U^{U} are listed in Table 1. We can confirm that an optimal solution with smaller number of members and larger V is obtained as U^{U} is decreased. However, the maximum height of the members in Figure 5(a) for $U^{\mathrm{U}} = 0.01$ is 56.439, which is unrealistic in comparison to the dimension of the frame. Furthermore, stress constraints should be satisfied for practical application. Hence, the displacement bound is conceived as an artificial parameter for controlling the number of members in an appropriate optimal topology.

We next solve Problem P3 using the solution in Figure 5(a) as the initial ground structure with reduced number of members. The optimal solution in Figure 5(a) is discretized to shorter members to obtain a smoothly curved frame. The vertical coordinates of nodes except the supports are also considered as design variables. Let Y_i^0 denote the y-coordinate of the ith node of the frame in Figure 5(a). The upper and lower bounds for Y_i are given as $Y_i^0 + 5$ and $Y_i^0 - 5$, respectively. Note that rather strict bounds are given to avoid an optimal shape with small height, because the endrope for the membrane sheet should be contained in the clamping member.

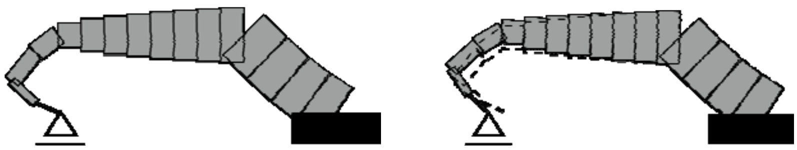

(a) (b)

Fig. 6: Optimal solution of Type 1 under stress constraints with variable nodal locations; (a) undeformed shape, (b) deformed shape

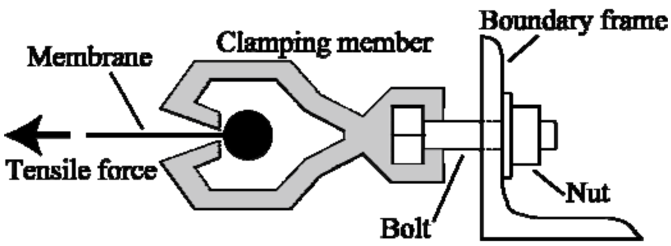

Fig. 7: Illustration of a self-fastening clamping member

Figure 6(a) shows the optimal shape with real scale, where $V = 1.7082 \times 10^4$. Figure 6(b) shows the deformed shape with magnification factor 20. As is seen, only the nodes near support 1 moves in the horizontal direction; thus, a vertical compressive force is applied from the frame to the support, and, accordingly, the clamping force increases as the tensile force of the membrane sheet increases. From this result, we can construct a self-fastening clamping member as illustrated in Figure 7.

4 Topology optimization of a clamping member with a tension adjustment bolt

4.1 Problem formulations

In Section 3, we presented a method for generating a clamping member that can automatically fasten the membrane sheet as the tensile force is increased. However, for application to the practical design of membrane structures, it is more desirable if the tensile force can be adjusted through additional forces to the clamping member as illustrated in Figure 8. Therefore, we next consider a problem with two loading conditions; i.e., the first load P_1 is applied by the vertical bolt to pull the membrane for adjustment of the tensile force, and the second load P_2 represents the tensile force of the membrane sheet.

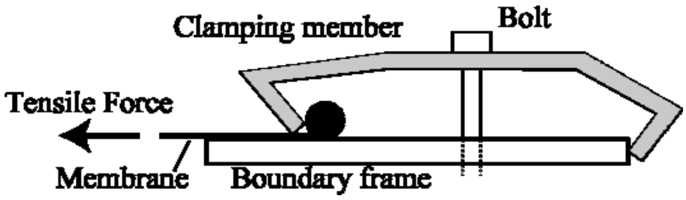

Fig. 8: Illustration a clamping member with tension adjustment bolt

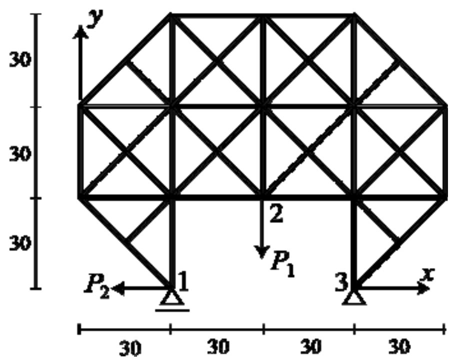

Fig. 9: A frame model (Type 2)

Let $U^{(1)}$ and $U^{(2)}$ denote the *x*-directional displacements of node (support) 1 in Figure 9 under specified static loads P_1 and P_2, respectively. We first minimize the total structural volume *V* without stress constraints to obtain a frame with small number of members. The lower bound $U^{(1)\mathrm{L}}$ (>0) is given to ensure capacity of adjustment by the bolt, and the lower bound $U^{(2)\mathrm{L}}$ (<0) is given for generating a frame with enough stiffness. A lower bound R^{L} is also given for the vertical (*y*-directional) reaction force $R_1^{(2)}(\mathbf{A})$ at support 1.

Then the optimization problem is formulated as follows:

P4: minimize $V(\mathbf{A})$ (6a)

subject to $U_1^{(1)}(\mathbf{A}) \geq U^{(1)\mathrm{L}}$ (6b)

$U_1^{(2)}(\mathbf{A}) \geq U^{(2)\mathrm{L}}$ (6c)

$R_1^{(2)}(\mathbf{A}) \geq R^{\mathrm{L}}$ (6d)

$\mathbf{A}^{\mathrm{L}} \leq \mathbf{A} \leq \mathbf{A}^{\mathrm{U}}$ (6e)

The optimal solution of Problem P4 is used as the new ground structure with small number of members. Since the number of members need not be reduced anymore, the displacement $U_1^{(1)}$ against P_1 can be directly maximized to obtain a good capacity of adjustment of membrane forces. Hence, we assign the stress constraints for both the states under P_1 only and under simultaneous application of P_1 and P_2, and solve the following problem adding the nodal coordinates **X** as variables.

P5: minimize $V(\mathbf{A}, \mathbf{X})$ (7a)

subject to $U_1^{(1)}(\mathbf{A}, \mathbf{X}) \geq U^{(1)\mathrm{L}}$ (7b)

$\left|\sigma_i^{(1)}(\mathbf{A}, \mathbf{X})\right| \leq \sigma^{\mathrm{U}} \quad (i = 1, \ldots, m)$ (7c)

$\left|\sigma_i^{(1)}(\mathbf{A}, \mathbf{X}) + \sigma_i^{(2)}(\mathbf{A}, \mathbf{X})\right| \leq \sigma^{\mathrm{U}} \quad (i = 1, \ldots, m)$ (7d)

$\mathbf{A}^{\mathrm{L}} \leq \mathbf{A} \leq \mathbf{A}^{\mathrm{U}}$ (7e)

$\mathbf{X}^{\mathrm{L}} \leq \mathbf{X} \leq \mathbf{X}^{\mathrm{U}}$ (7f)

where $\sigma_i^{(1)}$ and $\sigma_i^{(2)}$ are the stresses of member *i* against P_1 and P_2, respectively.

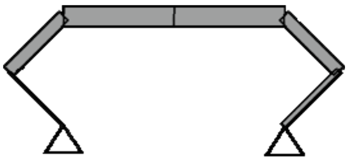

Fig. 10: Optimal solution of Type 2 under displacement constraint

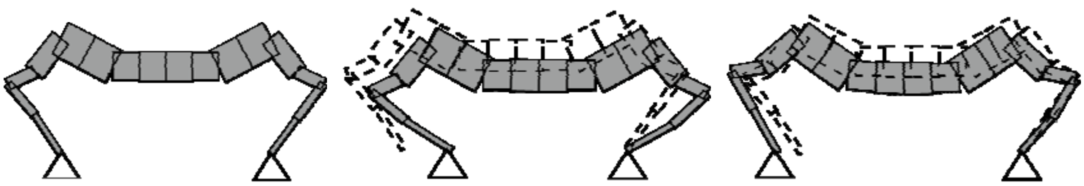

(a) (b) (c)

Fig. 11: Optimal solution of Type 2 under stress constraints; (a) undeformed shape, (b) deformed shape magnified by 10 after application of P_1; dotted line: undeformed shape, (c) deformed shape magnified by 10 after application of P_1 and P_2

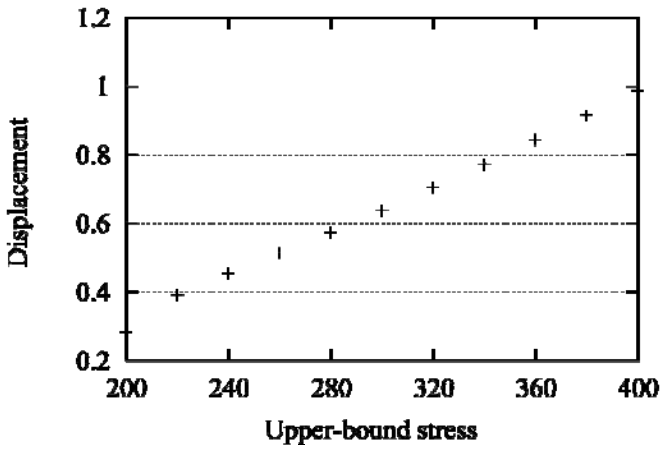

Fig. 12: Relation between upper-bound stress and displacement

4.2 Numerical examples

Consider a frame as shown in Figure 9. The load $P_1 = 300$ is first applied in the vertical direction at node 2. Then the *y*-directional displacement is fixed at node 2, and the load $P_2 = 300$ is applied in negative *x*-direction at support 1. Initial solutions are generated in the same manner as the examples in Sec. 3.

The solution of Problem P4 scaled by 1/5 for $U^{(1)\mathrm{L}} = 0.1$, $U^{(2)\mathrm{L}} = -0.01$, $R^{\mathrm{L}} = 200$, and $A_i^{\mathrm{U}} = 200$ for all members is shown in Figure 10, which has sufficiently small number of members. Problem P5 is next solved after subdivision of members, where the *y*-coordinates of nodes except the supports are also chosen as design variables, and their initial values and bounds are given in the same manner as the examples in Sec. 3.

The optimal solution is shown in Figure 11(a) with the real scale for the heights of members. The deformed shape against P_1 is shown in Figure 11(b). We can see from Figure 11(b) that the distance between the two supports decreases as the center node is displaced downward. Figure 11(c) shows the state after application of both P_1 and P_2 for the frame with fixed vertical displacement at node 2. As is seen, the roller support moves to the left, and, consequently, the diagonal member presses the support to increase the vertical reaction force.

Figure 12 shows the relation between the upper-bound stress σ^{U} and the displacement $U^{(1)\mathrm{L}}$ which is to be maximized. It can be confirmed from Figure 13 that we can have larger deformation if the stress constraints are relaxed.

5 Conclusions

A two-stage approach has been presented for configuration optimization of frames under stress constraints against static loads. It has been shown that an approximate optimal topology that has many members is obtained if stress constraints are assigned to all members. This result is similar to the truss topology optimization under stress constraints. Therefore, an approximate optimal topology with small number of members is obtained by relaxing the stress constraints and assigning an artificial displacement constraint. The optimal topology can be further optimized under stress constraints after sub-division of members, where the vertical coordinates of nodes are also considered as design variables.

It has been confirmed in the numerical examples that an optimal topology with a small number of members is obtained by assigning artificially small displacement constraint. This way, the well-known difficulty in topology optimization under stress constraints is successfully avoided.

Configuration optimization has been carried out to obtain self-fastening clamping members of membrane structures. The total structural volume is minimized under constraint on the reaction so that the clamping force increases as the result of increasing membrane tensile force. A shape of the device that pulls the membrane efficiently by applying vertical force through a bolt can also be found by optimization. This way, the total weight of a frame-supported membrane structure can be reduced, and the clamping force and the tension force can be maintained through optimization.

Acknowledgement

Financial support by Nohmura Foundation for Membrane Structure's Technology is gratefully acknowledged.

References

[1] Rahamia H, Kavehb A, and Gholipoura Y. Sizing, geometry and topology optimization of trusses via force method and genetic algorithm. *Eng. Struct.* 2008; **30**: 2360-2369.

[2] Fredricson H, Johansen T, Klarbring A, and Petersson J. Topology optimization of frame structures with flexible joints. *Struct. Multidisc. Optim.* 2003; **25**: 199-214.

[3] Saka MP. Optimum topological design of geometrically nonlinear single layer latticed domes using coupled genetic algorithm. *Comput. Struct.* 2007; **85**: 1635-1646.

[4] Ohsaki M. Optimization of Finite Dimensional Structures. CRC Press, Boca Raton, FL, 2010.

[5] Stolpe M and Svanberg K. A note on stress-constrained truss topology optimization. *Struct. Multidisc. Optim.* 2003; **25**: 62-64.

[6] Ohsaki M and Katoh N. Topology optimization of trusses with stress and local constraints on nodal stability and member intersection. *Struct. Multidisc. Optim.* 2005; **29**:190-197.

[7] Cheng G and Guo X. ε-relaxed approach in structural topology optimization, *Struct. Opt.* 1997; **13**:258-266.

[8] Duysinx P and Bendsøe MP. Topology optimization of continuum structures with local stress constraints. *Int. J. Numer. Methods Eng.* 1998; **43**:1453-1478.

[9] Bendsøe MP. Optimal shape design as a material distribution problem. *Struct. Opt.* 1989; **1**:193–202.

[10] Rozvany GIN, Zhou M, and Birker T. Generalized shape optimization without homogenization, *Struct. Opt.*, 1992; **4**:250-252.

[11] Gill PE, Murray W, and Saunders MA. SNOPT: An SQP algorithm for large-scale constrained optimization. *SIAM J. Optim.* 2002; **12**:979-1006.